J. Fluid Mech. (1984), *vol.* 146, *pp.* 169–179
Printed in Great Britain

'Sink' effect in a shock-induced boundary layer on attenuation

By B. E. L. DECKKER

Department of Mechanical Engineering, University of Saskatchewan, Saskatoon, Saskatchewan, Canada S7N 0W0

(Received 6 January 1984)

Experiments on shock-wave attenuation in a porous tube have shown that attenuation is a function of distance from the origin and the rate of cross-mass flow per unit area. It is a linear function of distance if the cross-mass flow rate per unit area is held constant. In a tube with solid walls the relationship between attenuation, mass extraction rate per unit area and distance is similar to that in a proous tube. The ratio of the local attenuation to the local cross-mass flow, or mass extraction rate, per unit area is the same linear function of distance in both sets of experiments. The mechanism of attenuation is therefore also identical.

1. Introduction

The attenuation of a shock wave propagating in a tube has been a problem of interest for a number of years and several publications relating to it have appeared from time to time (Glass & Martin 1955; Trimpi & Cohen 1955; Mirels 1956*a*, *b*; Holleyer 1956; Mirels & Braun 1957; Emrich & Wheeler 1958). The concept of the shock-induced boundary layer as an aerodynamic sink, contributing to attenuation of a shock wave, may have arisen from recognition of the fact that both the displacement thickness and momentum thickness of the boundary layer in shock-fixed coordinates are negative. Theoretically, however, it has been known from the generalization of Rayleigh's (1911) solution to the impulsively started plate problem that compressibility gives rise to a velocity component normal to the plate. This was the basis of Mirel's (1956*a*, *b*) treatment of the attenuation of a shock wave. Recently, the results of an experimental and theoretical investigation of attenuation of a shock wave in a porous tube in which the cross-mass flow rate was varied by partially sealing its external surface was reported (Deckker & Koyama 1983). At the time a tentative attempt was made to relate the mechanism of attenuation in a porous tube to the 'sink' effect in a tube with solid walls, and it was felt that a definitive demonstration of the 'sink' effect would be of value. In this paper, therefore, only a brief description of the important features of that investigation will be given and the experimental results reproduced as a starting point in the discussion.

2. Experimental considerations

A shock wave of strength $p_w/p_0 = 1.30$, p_w being the absolute pressure immediately behind the shock front and p_0 the undisturbed pressure, was generated in the cylindrical expansion duct of a shock tube. On arrival at the end of this duct, the central portion of the incident wave was transmitted through a coaxial porous tube 0.0232 m internal diameter and 1.353 m long. The reflected portion of the wave was

then cancelled by venting the expansion duct to the atmosphere through a peripheral gap in the plane of its partially closed end. In preliminary experiments, the required gap width was found to be 0.0175 m and the superimposition or net pressure of the quasi-steady flow entering the porous tube was equal to the pressure behind the incident wave. The duration of the constant pressure and particle velocity associated with the net wave was substantially greater than the time taken by the transmitted incident shock wave to traverse the porous tube. The porous tube was of sintered bronze with a uniform hole size of 0.0001 m and a wall thickness of 0.0036 m. It was supported along its length in a frame which was rigidly bolted to the end plate of the cylindrical expansion duct of the shock tube in which one end of the porous tube was located. A schematic drawing of the shock-tube arrangement is given in figure 1.

Six pressure taps, equidistantly spaced, were provided in the porous tube and are shown as CT1, ..., CT6 in that figure. Another pressure tap was provided at the position CT0 in the expansion tube 0.133 m from its partially closed end, where a piezoresistive pressure transducer (Endevco, 8507–15) was used to monitor the net pressure of the flow entering the porous tube. In each shock-tube firing, a second transducer (Endevco, 8507-15) was used in one of the locations CT1 or ... or CT6 in the porous tube. The transducer, which was 0.0023 m in diameter and 0.02 m long, was carried in a tubular sheath and when used in positions CT1, ..., CT6 the sheath was secured to the supporting frame with only the sensitive tip of the probe protruding through a hole in the tube wall. With this arrangement, there was no interference with the tube surface and no relative motion between the porous tube and transducer. The pressure taps not in use were blanked-off by inserts which were secured to the supporting frame in a manner similar to that of the transducer sheath.

Signals from the two pressure transducers were amplified (Bell & Howell 8-115) and fed into a high-speed recording system (Biomation 8100) operating in the 2-channel mode in which the information was stored. The amplified signal from the transducer in the porous tube was also fed into a storage oscilloscope (Tektronix 5113) so that the waveform could be visually monitored. The stored information was retrieved after each firing and plotted automatically (Hewlett-Packard 7001A). Measurements at each of the six positions CT1, ..., CT6 in the porous tube were repeated at least twice in each set of experiments to ensure that conditions within the porous tube were repeatable. Altogether five sets of experiments were carried out and about 100 successful shock-tube firings were made in the course of the investigation.

To examine the effect of cross-mass flow through the wall of the porous tube on the attenuation of a shock wave, the cross-mass flow was varied by partially sealing the external surface of the tube by wrapping a ribbon of impervious material in helical fashion on it. Four different helical pitches were used and, including the bare porous tube, there were five different surface configurations.

For each of these five surface configurations, the cross-mass flow rate $\dot{g}$ per unit area of internal surface was determined in separate experiments. These experiments were carried out under steady conditions for a range of decreasing pressures starting from the pressure equal to that behind the shock wave at entry to the porous tube. The cross-mass flow rates $\dot{g}$ determined in this way were approximated by polynomial expressions in powers of the pressure ratio p_w/p_0, which were used afterwards in the theoretical analysis of attenuation (Deckker & Koyama 1983). These equations are reproduced in table 1. The assumption underlying these experiments was that conditions associated with the passage of the shock could be treated as a succession

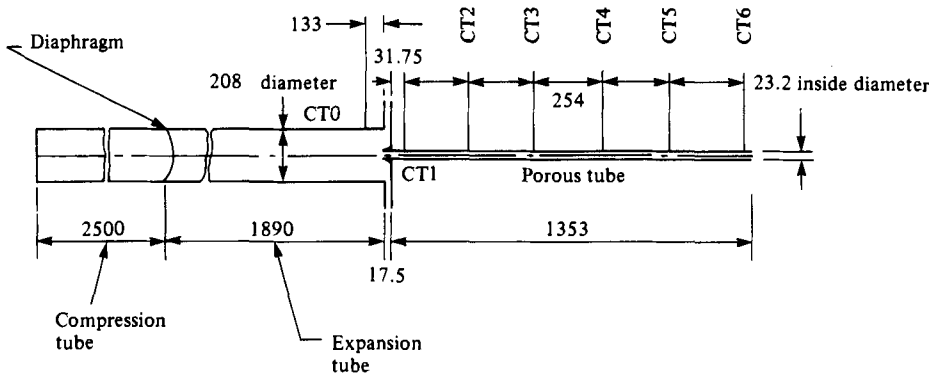

FIGURE 1. Schematic drawing of shock tube (dimensions in mm).

Curve no.	Description of tube surface	Equation of cross-mass flow rate $\dot{g}$ per unit area of internal surface
1	bare	$-1.335+1.650\overline{p}$
2	partially sealed	$-2.195+2.200\overline{p}$
3	partially sealed	$-188.45+620.35\overline{p}-765.95\overline{p}^2+419.74\overline{p}^3-85.82\overline{p}^4$
4	partially sealed	$-116.85+389.16\overline{p}-486.90\overline{p}^2+270.75\overline{p}^3-56.23\overline{p}^4$
5	partially sealed	$26.68-82.44\overline{p}+93.88\overline{p}^2-46.95\overline{p}^3+8.88\overline{p}^4$

TABLE 1. Cross-mass flow-rate equations for porous tube. $\overline{p} = p_w/p_0$, where p_w is pressure behind shock wave. Curve numbers refer to figure 2(*a*). Extent of tube surface sealed increases from curve 2 to curve 5.

of quasi-steady states and that for each state the cross-mass flow $\dot{g}$ would be commensurate with the local pressure p_w behind the shock, the ambient pressure p_0 at the tube surface, and the effective pore area of the tube.

3. Experimental results and discussion

The results of the experiments reported in Deckker & Koyama (1983) are reproduced in figure 2(*a*). In this figure, the local pressure p_w behind the shock wave and the distance x from the origin at which it is measured are expressed non-dimensionally as p_w/p_0 and x/d_0 respectively, d_0 being the internal diameter of the tube. Between the origin and $x/d_0 = 10$ the rate of attenuation of the shock wave for the five different surface configurations is higher than when $x/d_0 > 10$. This is attributed to interstitial leakage internally in the tube wall, since the air filling the void volume would be atmospheric and at a lower pressure than that behind the shock when it enters the porous tube. The relatively lower rates of attenuation between $x/d_0 = 10$ and $x/d_0 = 50$ are believed to be associated with conditions in the tube wall that are closer to its true 'porosity', unaffected by interstitial leakage. In fact, in this range of x/d_0, agreement between the experimental results and those obtained theoretically was found to be satisfactory when the cross-mass flow rates $\dot{g}$ per unit area given in table 1 were used (Deckker & Koyama 1983). To offset the effects of interstitial leakage, those parts of the experimental curves lying beyond $x/d_0 = 10$ have been extrapolated to the origin $x/d_0 = 0$, and the values of p_w/p_0 so obtained

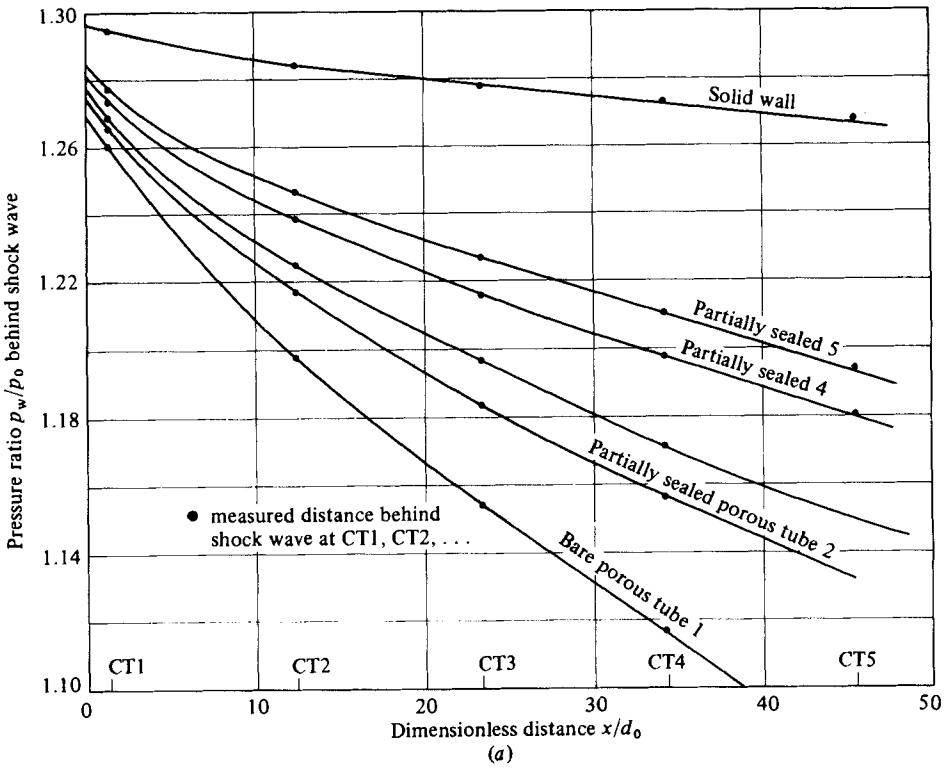

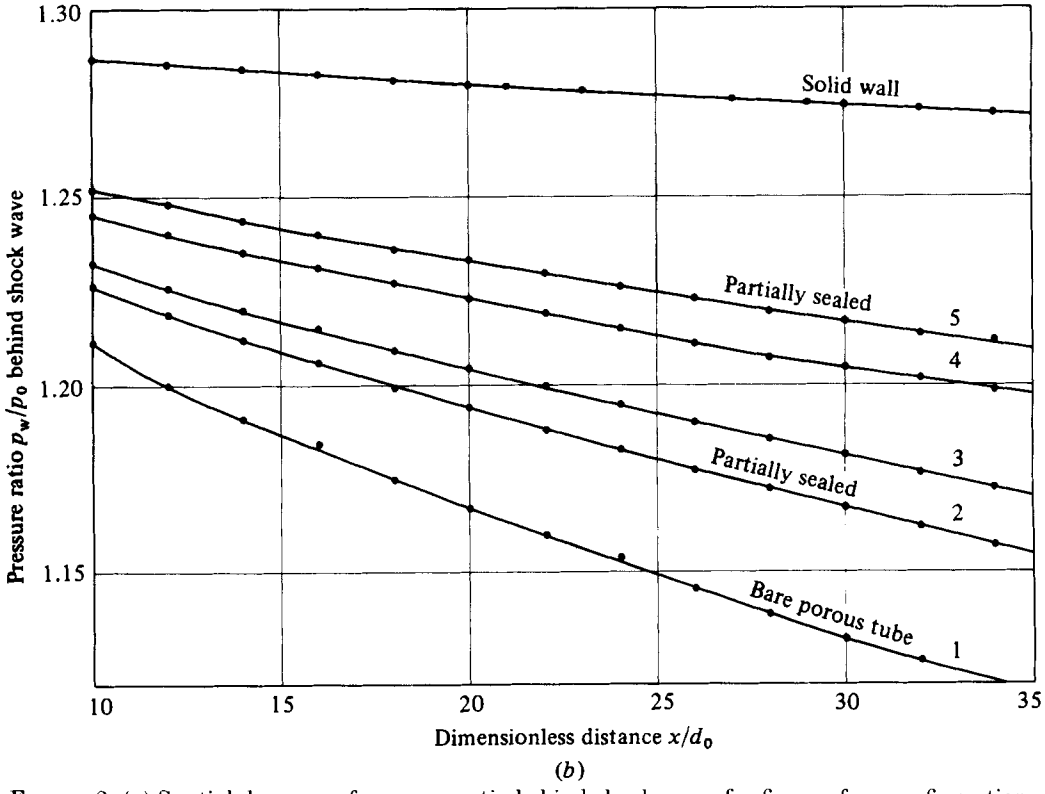

FIGURE 2. (*a*) Spatial decrease of pressure ratio behind shock wave for five surface configurations of a porous tube and for a tube with solid walls. (*b*) Spatial decrease of pressure ratio behind shock wave between $x/d_0 = 10$ and $x/d_0 = 35$.

Curve no.	Description of surface	Pressure ratio p_w/p_0 at $x/d_0 = 0$
1	bare	1.261
2	partially sealed	1.264
3	partially sealed	1.267
4	partially sealed	1.272
5	partially sealed	1.278

TABLE 2. Initial pressure ratios of shock wave

are considered to be the initial shock strengths for the purposes of this paper. These values of p_w/p_p are reproduced in table 2.

Those parts of the curves in figure 2(*a*) lying between $x/d_0 = 10$ and $x/d_0 = 34$ have been reproduced to a larger scale in figure 2(*b*), and data from this figure have been used in the development that follows.

In figure 2(*b*), for lines of constant x/d_0 equal to 12, 16, 20, etc., local pressure ratios p_w/p_0 were found along each of the curves labelled 1, 2, ..., 5 and using the initial values of p_w/p_0 from table 2, the dimensionless attenuation $\Delta p_w/p_0$ (that is, the difference of the initial value of p_w/p_0 and the local values along each curve) was determined. Also for these local values of p_w/p_0 along each curve, the corresponding cross-mass flow rates $\dot{g}$ were calculated using the expressions given in table 1. Pairs of values of $\Delta p_w/p_0$ and $\dot{g}$ for constant values of x/d_0 obtained in the manner described have been plotted in figure 3(*a*). The abscissa in that figure is the cross-mass flow rate $\dot{g}$ per unit area in kg m^{-2} s^{-1}, and the parameter is the dimensionless length x/d_0. The five arrays of points correspond to the five surface configurations used, that on the right is for the bare surface, curve 1 in figure 2(*b*), and that on the left corresponds to curve 5 in that figure. The information represented by mean curves through the experimental points have been replotted in figure 3(*b*) in a coordinate framework of dimensionless attenuation $\Delta p_w/p_0$ and dimensionless length x/d_0, with the cross-mass flow rate $\dot{g}$ per unit area as the parameter. The linear dependence of attenuation on distance from the origin when $\dot{g}$ is constant is intuitively reasonable. The linearity is lost, as may be seen in figure 2(*a*) or 2(*b*), because of the dependence of $\dot{g}$ on the pressure for the given uniform 'porosity' represented by each of the five surface configurations. The linear relationship between attenuation and distance cannot be reproduced experimentally unless the 'porosity' of the tube is made variable along its length so as to satisfy the condition $\dot{g}$ = constant as the shock wave becomes attenuated.

Superimposed on figure 3(*b*) is the curve of dimensionless attenuation, in a tube with solid walls, of a shock wave of initial strength $p_w/p_0 = 1.30$, which has been taken from figure 2(*a*). The tube used in this experiment was of the same internal diameter (0.0232 m) and length (1.353 m) as the porous tube. In the coordinate framework of figure 3(*b*), straight lines drawn from the origin to points along the attenuation curve represent mass extraction rates per unit area from the free stream into the induced boundary layer similar to the cross-mass flow rates $\dot{g}$ per unit area, in the porous tube. It is evident that these mass extraction rates per unit area decrease at further distances from the origin. This variation is intuitively reasonable, since the flux of mass from the free stream into the induced boundary layer is likely to decrease as the pressure behind the shock wave decreases with distance from the origin as a result of attenuation. In figure 3(*c*) the scale of dimensionless attenuation has been enlarged

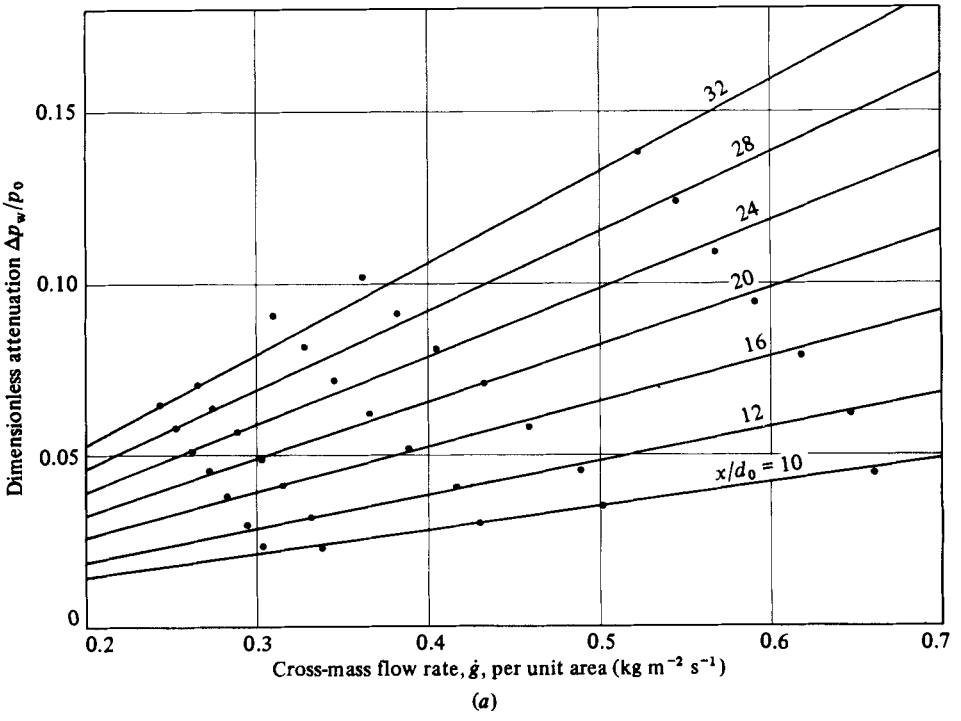

FIGURE 3. (*a*) Dimensionless attenuation of shock wave in a porous tube for five surface configurations as a function of cross-mass flow rate $\dot{g}$ per unit area when x/d_0 is held constant. (*b*) Dimensionless attenuation of shock wave in a porous tube as a function of dimensionless distance when $\dot{g}$ is held constant. The dimensionless attenuation of the shock wave in a tube with solid walls is shown superimposed. (*c*) Dimensionless attenuation (to enlarged scale) of shock wave in a tube with solid walls from (*b*) showing lines of constant mass extraction rate per unit area analogous to $\dot{g}$ in a porous tube through points on curve.

and the lines $\dot{g} = 0.1$ kg m^{-2} s^{-1} and $\dot{g} = 0.2$ kg m^{-2} s^{-1} from figure 3(*b*) have been superimposed on it. Straight lines joining the origin of coordinates to points along the experimental attenuation curve when interpolated linearly between $\dot{g} = 0$ and $\dot{g} = 0.2$ kg m^{-2} s^{-1} give numerical values of the mass extraction rates per unit area corresponding to the local dimensionless attenuation of the shock wave. In the range of x/d_0 shown in figure 3(*c*) these rates vary between 0.162 kg m^{-2} s^{-1} at $x/d_0 = 1$ and 0.082 kg m^{-2} s^{-1} at $x/d_0 = 34$.

In figure 3(*a*) , if the local dimensionless attenuation p_w/p_0 for constant values of x/d_0 in the porous tube are divided by the corresponding values of $\dot{g}$ and the results plotted against the dimensionless length x/d_0, the results are found to lie on a straight line through the origin of coordinates, as in figure 4. The short vertical lines in that figure indicate the spread of these results. It is interesting that, for the shock wave in the tube with solid walls, if the local dimensionless attenuations for different values of x/d_0 from figure 3(*c*) are divided by the corresponding mass extraction rates per unit area, the results lie on the same line in figure 4. The inference to be drawn from this result is that the mechanism of attenuation is the same in the porous tube as in the tube with solid walls, namely mass extraction from the through flow or free stream.

While it is evident that mass extraction from the free stream has a significant effect on the motion of a shock wave in a tube with either porous walls or solid walls, the

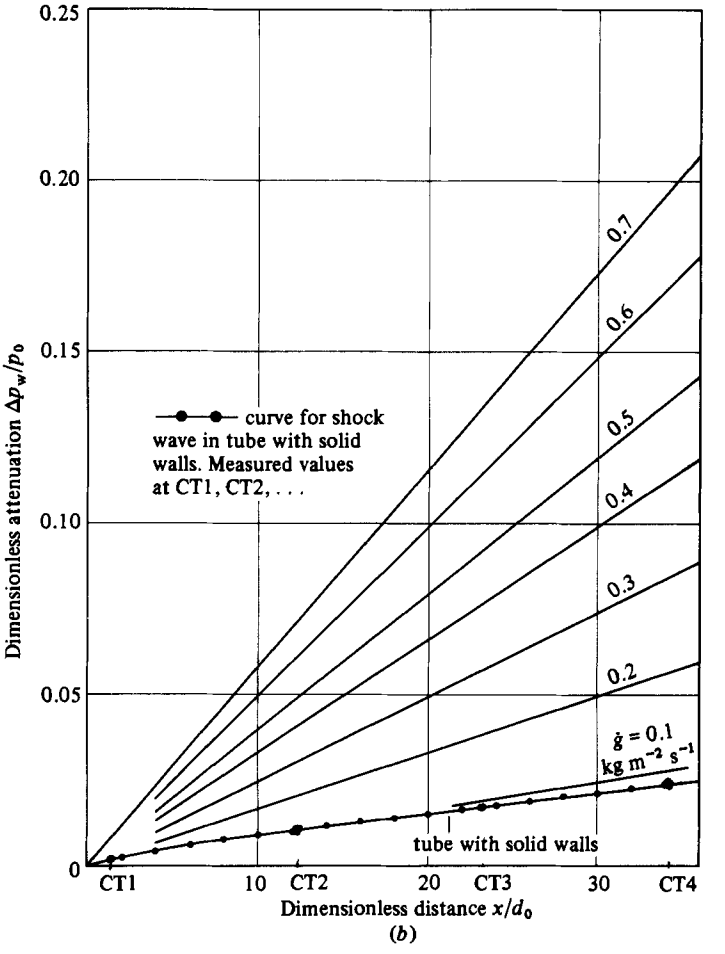
0.25
0.20
0.15
0.10
0.05
0
Dimensionless attenuation $\Delta p_w/p_0$
curve for shock wave in tube with solid walls. Measured values at CT1, CT2, . . .
0.7
0.6
0.5
0.4
0.3
0.2
$\dot{g} = 0.1$ kg m^{-2} s^{-1}
tube with solid walls
CT1
10
CT2
20
CT3
30
CT4
Dimensionless distance x/d_0

(*b*)

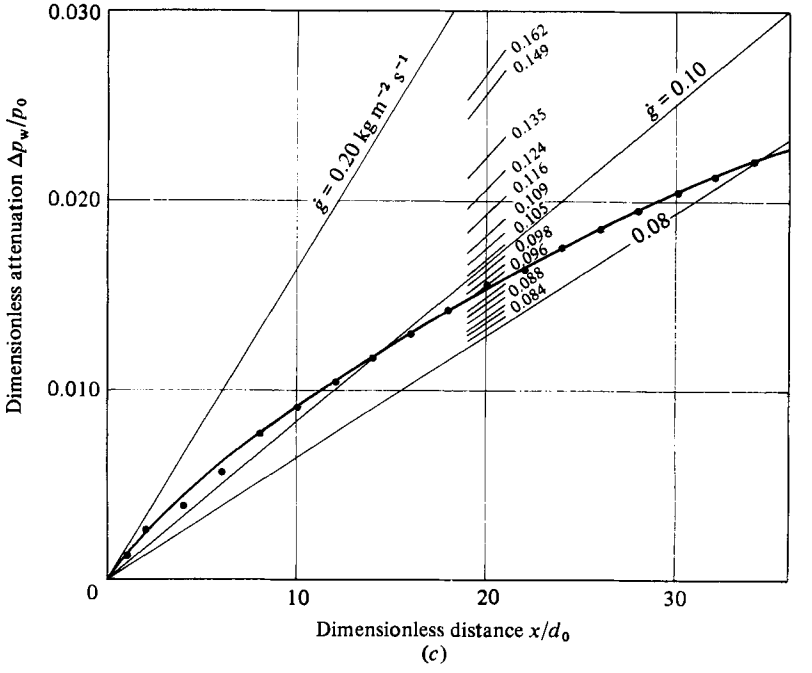
0.030
0.020
0.010
0
Dimensionless attenuation $\Delta p_w/p_0$
$\dot{g} = 0.20$ kg m^{-2} s^{-1}
0.162
0.149
0.135
0.124
0.116
0.109
0.105
0.098
0.096
0.088
0.084
$\dot{g} = 0.10$
0.08
10
20
30
Dimensionless distance x/d_0

(*c*)

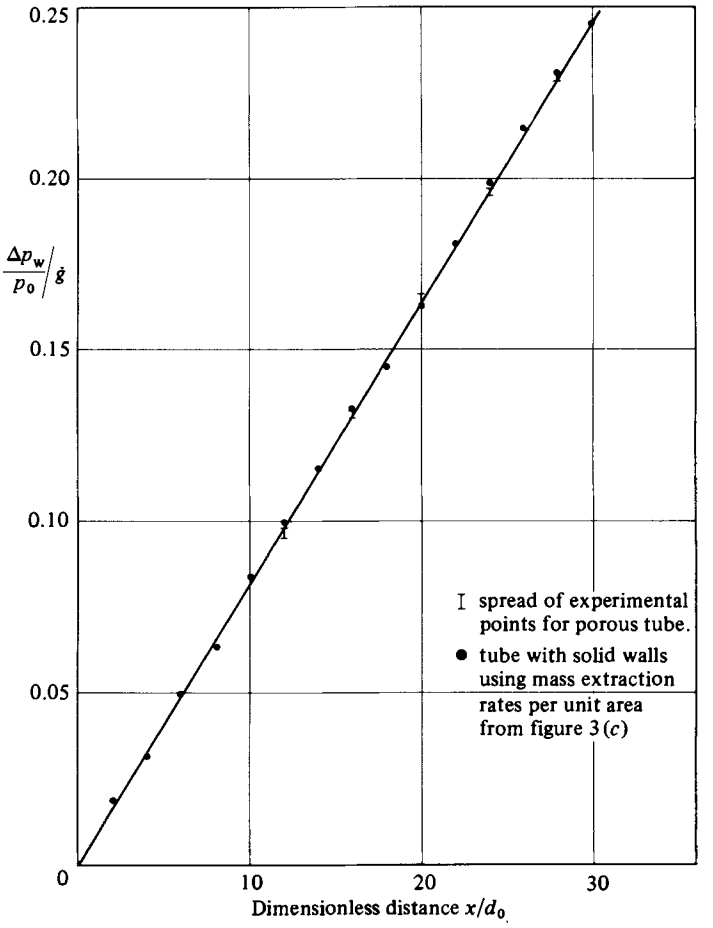

FIGURE 4. Plot of ratio $(\Delta p_w/p_p)/\dot{g}$ for a porous tube and for a tube with solid walls using analogous values of $\dot{g}$ from figure 3(*c*).

preceding results do not explain its precise role. The question that is raised here is whether attenuation of a shock wave stems directly from mass extraction or whether it is due indirectly to mass extraction which gives rise to rarefaction waves that propagate in all directions from the tenuous edge of the boundary layer. Rarefaction waves propagating in the direction of the flow catch up with the shock front and attenuate it. This is Mirels' hypothesis. The present author's results, which are based on the cross-mass flow rates $\dot{g}$ and the analogous mass extraction rates in the tube with solid walls, come essentially from a quasi-steady analysis in which the unsteadiness is due to attenuation of the shock wave itself. On the basis of this assumption, attenuation in the porous tube, and in the tube with solid walls, should be amenable to prediction by a simple thermodynamic analysis using the empirical values of $\dot{g}$ in the one case and the analogous mass extraction rates in the other.

If a small control volume $\frac{1}{4}\pi d_0^2 \Delta x$, where Δx is its axial extent and d_0 the internal diameter of the tube, is fixed in the moving shock wave, its subsequent motion may be followed in a stepwise manner. At the beginning of each step, the speed of the shock wave and the properties behind it have been calculated on the basis of the local pressure using the one-dimensional equations. At the end of the step, the decrease

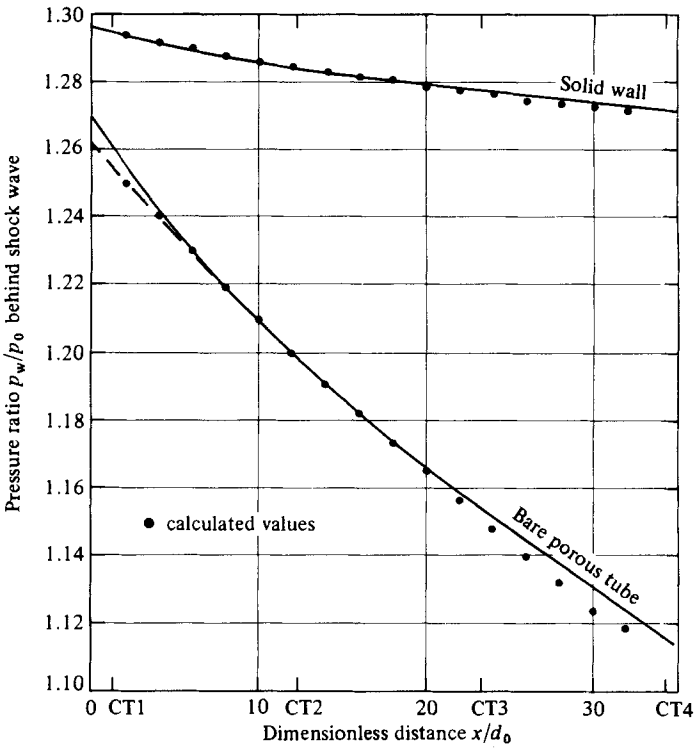

FIGURE 5. Spatial decrease in pressure ratio behind shock wave in a bare porous tube and in a tube with solid walls showing comparison between experimental curves, from figure 2(*a*), and calculated values from quasi-steady analysis.

in pressure is found from the change in the thermodynamic state of the residual air in the control volume after mass extraction. In this way, good agreement has been obtained with the experimental curves for the bare porous tube (curve 1 in figure 2*a*) and for the tube with solid walls, as may be seen in figure 5. These results have been obtained using the empirical equation for $\dot{g}$ for the bare porous tube from table 1 and the mass extraction rates per unit area for the tube with solid walls obtained from figure 3(*c*). The effective area through which mass extraction occurred was taken in both cases to be 0.72 times the circumferential area of the control volume, which is $\pi d_0 \Delta x$. If the transverse surfaces of the control volume are assumed to be impervious to material fluxes, the theoretical area for mass transfer would be $0.50\pi d_0 \Delta x$. The increase in this factor from 0.5 to 0.72 reflects the fact that some mass transfer must occur through the downstream transverse control surface. This is reasonable, since the pressure at any of the positions CT1, CT2, ..., CT6 decreases behind the shock wave as the latter sweeps past it. Thus a favourable pressure gradient for mass transfer exists at the downstream control surface. In the porous tube, in particular, the rate of decrease in pressure is fairly high.

The kind of analysis postulated excludes any interaction between the induced boundary layer and the contact surface in so far as attenuation of the shock wave itself is concerned. Clearly there must be a net exchange of mass along the length of the boundary layer at its interface with the free stream, however tenuous that may be, which could influence the contact surface in a manner similar to that at the shock

wave itself. In the apparatus used, the contact surface is remote from the shock wave in the porous tube, or in the tube with solid walls, and would be located in the cylindrical expansion duct of the shock tube (figure 1).

4. Conclusions

Measurements of the attenuation ratio $\Delta p_w/p_0$ of weak shock waves in a porous tube have shown that the ratio of the local attenuation to the local cross-mass flow rate $\dot{g}$ per unit area is a linear function of the dimensionless distance x/d_0 from the origin. Different 'porosities' have been simulated by partially masking the surface of the porous tube, and in each case the cross-mass flow per unit area is known as a function of the local pressure ratio p_w/p_0 behind the shock wave. For the bare porous tube and four other masked surface configurations the linear relationship between the ratio $(\Delta p_w/p_0)/\dot{g}$ and the distance x/d_0 is the same.

For a shock wave in a tube with solid walls, the local attenuation $\Delta p_w/p_0$ has been related to a local mass extraction rate per unit area, analogous to $\dot{g}$ for the porous tube. The ratio of these two quantities and the dimensionless length x/d_0 have been found to be related in precisely the same way as for the porous tube. This coincidence clearly points to a common mechanism of attenuation, namely mass extraction from the through flow or free stream.

On the basis of the known value of $\dot{g}$ as a function of the local shock-pressure ratio p_w/p_0 and starting from the value of p_w/p_0 at the origin in the bare porous tube, the experimental curve for the decrease in p_w/p_0 has been reproduced over the greater part of the tube by a simple thermodynamic analysis. A similar analysis has been found to reproduce the experimental curve for the tube with solid walls, using the mass extraction rates per unit area, analogous to $\dot{g}$ in the porous tube, found from the experimental data. In the case of the porous tube, and the tube with solid walls, the same value of the effective surface area, namely $0.72\pi d_0 \Delta x$, has been used.

The success obtained by using a simple thermodynamic analysis to reproduce the two experimental curves under conditions so different as the bare porous tube and the tube with solid walls raises some doubt as to the need to evoke a role for wave action in the free stream, generated as a result of mass extraction, as the mechanism of attenuation (Mirels & Braun 1957).

The experiments described in this paper demonstrate clearly the effects of mass extraction on attenuation of a shock wave in a tube with solid walls, but the associated analysis does not predict what the attenuation would be when only conditions at entry to a tube are given. However, it remains to be seen whether, using a time-dependent numerical scheme for the fully developed laminar, or turbulent, boundary layer on a plate behind a shock wave whose strength is decreased by the mass extraction rate per unit area calculated from the transverse component of velocity at the edge of the boundary layer will yield results similar to those obtained here.

The experimental work reported was carried out in the Mechanical Engineering Department at the University of Saskatchewan under a grant-in-aid from the Natural Sciences and Engineering Research Council. The author thanks Dr H. S. Koyama of Tokyo Denki University for permission to use the experimental results.

REFERENCES

DECKKER, B. E. L. & KOYAMA, H. S. 1983 Paper presented at 14th Intl Symp. on Shock Tubes and Waves, University of Sydney, Australia, 15–18 August 1983 (to be published).

EMRICH, R. J. & WHEELER, D. B. 1958 *Phys. Fluids* **1**, 14.

GLASS, I. I. & MARTIN, W. A. 1955 *J. Appl. Phys.* **26**, 113.

HOLLEYER, R. N. 1956 *J. Appl. Phys.* **27**, 254.

MIRELS, H. 1956*a* *NACA Tech. Note* 3278.

MIRELS, H. 1956*b* *NACA Tech. Note* 3712.

MIRELS, H. & BRAUN, W. H. 1957 *NACA Tech. Note* 4021.

RAYLEIGH, LORD 1911 *Phil. Mag.* **21**, 697.

TRIMPI, R. L. & COHEN, N. B. 1955 *NACA Tech. Note* 3375.